 CMES, vol.39, no.1, pp.29-47, 2009

Estimation of thermo-elasto-plastic properties of thin-film mechanical properties using MD nanoindentation simulations and an inverse FEM/ANN computational scheme

D. S. Liu[1] **and C.Y. Tsai**[1]

Abstract: Utilizing a thin copper substrate for illustration purposes, this study presents a novel numerical method for extracting the thermo-mechanical properties of a thin-film. In the proposed approach, molecular dynamics (MD) simulations are performed to establish the load-displacement response of a thin copper substrate nanoindented at temperatures ranging from 300∼1400 K. The load data are then input to an artificial neural network (ANN), trained using a finite element model (FEM), in order to extract the material constants of the copper substrate. The material constants are then used to construct the corresponding stress-strain curve, from which the elastic modulus and the plastic level of the thin copper film are subsequently derived. The results show that both the elastic modulus and the plastic level decrease more than 30% as the simulation temperature increases from 300 K to 900 K. Comparing the result obtained from the ANN scheme for the elastic modulus of the thin copper film at room temperature with that obtained experimentally from a micro-force indentation test, it is found that the numerically-derived value (174 GPa) is higher than that obtained experimentally (145 GPa) [Pelletier, Krier, Cornet and Mille (2000)]. The discrepancy between the two sets of results is thought to arise primarily as a result of the high strain rate employed in the MD simulations and the assumption of a perfect, defect-free monocrystalline copper microstructure.

Keywords: Thin film, Thermo-mechanical properties, Molecular dynamics (MD), Artificial neural network (ANN), Finite element method (FEM).

1 Introduction

Thin films and coatings with thicknesses as little as several nanometers are widely applied in a variety of applications nowadays, including micro-electro-mechanical

[1] Department of Mechanical Engineering, National Chung Cheng University, 168, University Rd., Ming-Hsiung, Chia-Yi, 621, Taiwan, R.O.C.

systems (MEMS), nano-electro-mechanical systems (NEMS), semiconductors, magnetic devices, optical films, and so forth. Many of the thin film applications, however, may experience elevated temperatures. For effective designing and accurate evaluation of the structure integrity, quantitatively characterizing the thermal mechanical properties of the thin film is increasingly demanded for the applications.

Although various methods exist for characterizing the mechanical properties of a material at the nanoscale, depth-sensing indentation at ultra-low loads, commonly referred to as nanoindentation, is a particularly effective means of measuring the hardness and elastic modulus of thin films and coatings [Oliver and Pharr (1992)]. In the nanoindentation method, the mechanical properties of the thin film are determined by converting the force-displacement curves generated during the loading and unloading steps into a corresponding stress-strain curve. However, obtaining meaningful experimental results becomes increasingly difficult as the characteristic size of the thin film reduces due to the relatively greater effect of equipment limitations such as the machine resolution, the tip-rounding effect, the signal-to-noise ratio of the detection system, and so on. Moreover, environmental factors such as the ambient temperature and humidity have a significant effect on the mechanical properties of typical thin-film materials, but are difficult to quantify experimentally. Accordingly, various researchers have enhanced the original nanoindentation test procedure to improve the reliability of its results [Jayaraman, Hahn, Oliver, Rubin and Bastias (1998); Bouzakis, Vidakis (1999); Pelletier, Krier, Cornet and Mille (2000); Bouzakis, Michailidis and Erkens (2001); Chen, Yuan and Wittmann (2002); Bouzakis, Michailidis, Hadjiyiannis, Skordaris and Erkens (2003)]. For example Jayaraman, Hahn, Oliver, Rubin and Bastias (1998) developed an ultra-low-load indentation test procedure and obtained uniaxial stress-strain curves using a variety of indenter shapes. Other researchers have employed finite element method (FEM) techniques to optimize the nanoindentation experimental procedure or to support the evaluation of the nanoindentation test results. For example, Pelletier, Krier, Cornet and Mille (2000) assumed the thin-film material to be characterized by a bilinear stress-strain relationship and employed FEM simulations to determine the optimal tip radius of the indenter. Although the FEM schemes presented in the literature enable the plastic behavior of the thin film to be inversely extracted from the experimental load-displacement curve, they assume the nanoindentation test to be performed at room temperature. However, as discussed above, the mechanical properties of thin-film systems are highly sensitive to the temperature conditions, and thus some form of technique is required to account for both the indenter-to-film interactions and the temperature dependency of the mechanical properties of the indented film.

Molecular dynamics (MD) simulations provide a powerful technique for measuring

the materials strength [Li and Yip (2002); Liang, Woo, Huang, Ngan and Yu (2004); Nair, Farkas and Kriz (2008)] and evaluating the temperature dependency of the physical quantities of interest in nanoindentation tests [Yu, Adams, Hector (2002)]. Utilizing a three-dimensional MD model, Fang, Weng and Chang (2003) showed that both the elastic modulus and the hardness of thin films reduce as the temperature increases. However, it was noted that the numerically-derived value of the elastic modulus was around 256% higher than that obtained experimentally from a micro-force tensile test performed at room temperature. The authors suggested that the difference between the two sets of results could be attributed to scale differences and the simulation's assumption of a perfect defect-free monocrystalline copper, whereas the experimental workpieces may contain a variety of defects. Hsieh, Ju, Li and Hwang (2004) performed a series of simulations at temperatures ranging from 300$\sim$1300 K to analyze the correlation between the system temperature and the nanoindentation results and to identify the critical temperature for the transition of plastic flow mechanism in the copper substrate. Fang, Chang and Weng (2006) showed that MD simulations were an ideal means of identifying the optimal values of the applied load, the indentation depth, the holding time and the temperature when performing the nanoindentation of gold and platinum thin films.

The current study presents a numerical method comprising MD simulations, a finite element (FE) model and an artificial neural network (ANN) to extract the thermo-mechanical properties of a thin monocrystalline copper substrate. In the proposed approach, MD simulations are performed to establish the load-displacement curves corresponding to nanoindentation tests performed at temperatures ranging from 300 $\sim$ 1400 K. Utilizing the MD simulation results to define an appropriate parameter domain, FE simulations are then performed to construct a further series of load-displacement curves, which are then discretized using a uniform displacement interval and used to train an ANN designed to predict the material constants of the indented material. Having trained the ANN, and verified its performance, the load data obtained from the MD simulations are supplied to the ANN in order to determine the corresponding values of the material constants. Finally, the predicted values of these constants are used to construct the corresponding stress-strain curve, from which the elastic modulus and plastic level of the indented copper substrate are then obtained. The flowchart diagram of the developed numerical method described above to determine the thermo-mechanical properties of a thin film is demonstrated in Figure 1. The validity of the inversely-derived stress-strain curves can be confirmed by using the associated stress-strain data to recreate the corresponding FE load-displacement curves and then comparing these curves with those obtained from the MD simulations.

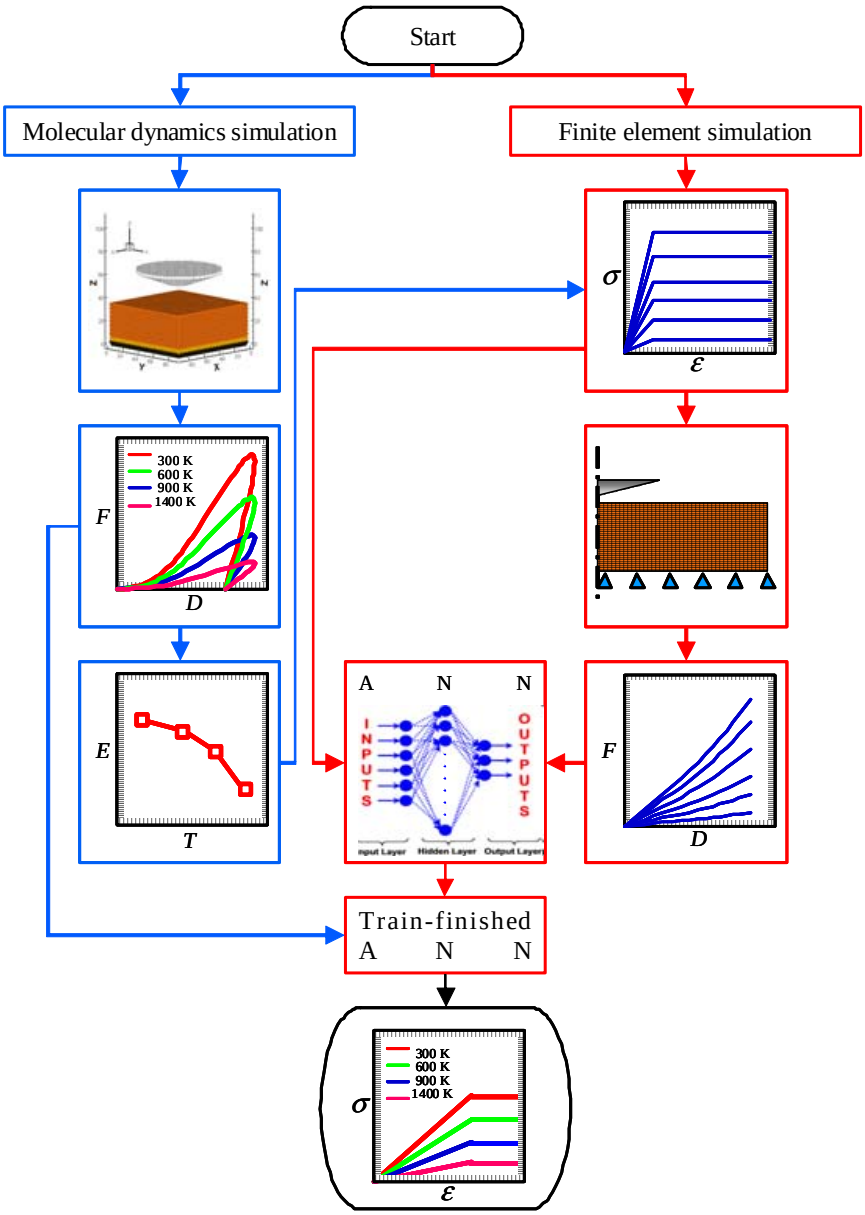

Figure 1: Flowchart diagram to determine a thin film thermo-elastic-plastic stress strain curves, based on the FEM/ANN and MD evaluation of nanoindentation results.

2 Molecular dynamics simulation

The MD simulations conducted in this study were performed using self-written code, and modeled the nanoindentation of a fcc crystalline copper substrate using either a rigid diamond tip or a conical indenter. The simulations commenced by validating the proprietary code by simulating the nanoindentation of a copper substrate at a temperature of 900 K and then comparing the simulation results for the load-displacement curve with the numerical results presented in [Hsieh, Ju, Li and Hwang (2004)]. The validation trial was performed using the MD model shown schematically in Figure 2. In this model, the copper substrate, with dimensions of 72.3 Å $\times$ 72.3 Å $\times$ 36.2 Å, consists of 20 layers of atoms with 800 atoms in each layer, giving a total of 16000 atoms. The upper 16 layers constitute a thermal control layer and are used to maintain the substrate at the specified temperature. Meanwhile, the lower two layers form a fixed boundary which prevents the substrate from moving in the z-direction during the indentation process. Finally, the two layers between the thermal control layer and the fixed boundary layer contain free-motion atoms and are designed to alleviate the artificial stiffness effect introduced by the fixed layer and to allow dislocation motions to take place within the deformed substrate. The validation test was performed using a diamond indenter tip comprising a total of 4552 carbon atoms. In performing the simulation, the indenter was assumed to be perfectly rigid and hence its deformation was neglected during the indentation process. In the simulation, periodic boundary conditions were imposed in the x- and y-directions and the time step was specified as $\Delta t = 1$ fs. Prior to the indentation process, the tip was positioned at a height of 10 Å above the substrate surface in order to prevent an attractive force between them. An equilibration process was then performed for 20000 time steps to achieve a steady-state system temperature of 900 K. The indenter was then moved through a total distance of 25 Å in the downward direction at a constant speed of 100 m/s. Having reached the indenter at the position of maximum load, it was returned to its original position at the same speed.

In the simulations, the positions and velocities of the atoms in the indenter and copper substrate at each time step were computed from the corresponding data in the previous step using the Gear's fifth-order predictor-corrector method [Haile (1992)]. The interactions between the copper atoms in the substrate were modeled using the Tight-Binding potential function, i.e.

$$E = \sum_{i=1}^{N} \left\{ A e^{-p\left(r_{ij}/r_0 - 1\right)} - \left[\sum_j \xi^2 e^{-2q\left(r_{ij}/r_0 - 1\right)} \right]^{1/2} \right\}, \tag{1}$$

where r_{ij} is the distance between copper atoms i and j, r_0 is the first-neighbor dis-

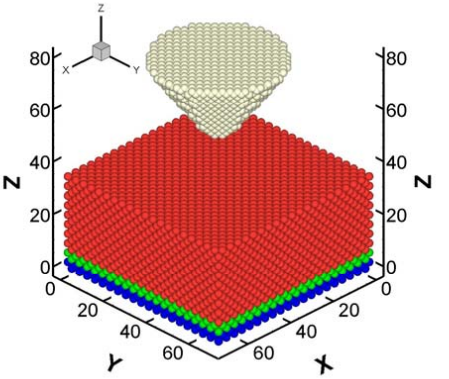

Figure 2: MD model used in validation test.

tance in the fcc lattice, and A, ξ, p and q are constants with values of $0.0855\,(eV)$, $1.224\,(eV)$, 10.906 and 2.278, respectively.

The interactions between the copper atoms in the substrate and the carbon atoms in the indenter were modeled using the Morse potential, i.e.

$$\phi(r) = D\left(e^{-2\alpha(r-r_0)} - 2e^{-\alpha(r-r_0)}\right), \tag{2}$$

where r is the length of the copper-carbon bond and D, α and r_0 denote the cohesive energy, the elastic modulus, and the atomistic distance under equilibrium conditions, respectively. The values assigned to D, α and r_0 in the present simulations are summarized in Table 1 [Maekawa and Itoh (1995)].

Table 1: Parameters used in Morse potential for carbon-copper binding

Parameter	Cu–Cu	Cu–C	C–C
$D\,(eV)$	0.3429	0.1	2.423
$\alpha\left(10^{10}m^{-1}\right)$	1.3588	1.7	2.555
$r_0\left(10^{-10}m\right)$	2.6260	2.2	2.522

Having validated the MD code, a series of numerical simulations was performed to investigate the effect of the system temperature on the thermo-mechanical properties of the thin copper film. Figure 3 presents a schematic illustration of the

corresponding MD model. As shown in the figure, the shape of the indenter used in the validation trial was modified. The tip radius of the indenter was specified as 10 Å, while the half-angle was assigned a value of 60°. Therefore substantially reduces the complexity of the 2D/3D axisymmetric modeling task. Furthermore, the use of a blunt tip reduces the indentation depth required to obtain the material properties of the copper film and therefore minimizes the effect of the underlying substrate material on the measured properties of the thin-film. The simulations were performed at temperatures ranging from $300 \sim 1400$ K using a copper substrate measuring 90.4 Å $\times$ 90.4 Å $\times$ 72.3 Å and containing a total of 50000 atoms. Prior to each simulation, the indenter was positioned at a height of 20 Å above the substrate surface and was then moved through a vertical distance of 28 Å at a rate of 50 m/s. The indenter was reached at the position of maximum load and was then returned to its original position. Note that in performing these simulations, both the indentation depth and the indenter speed were deliberately assigned lower values than those used in the validation trial since the indentation process was performed using a blunt conical indenter rather than a sharp diamond tip indenter.

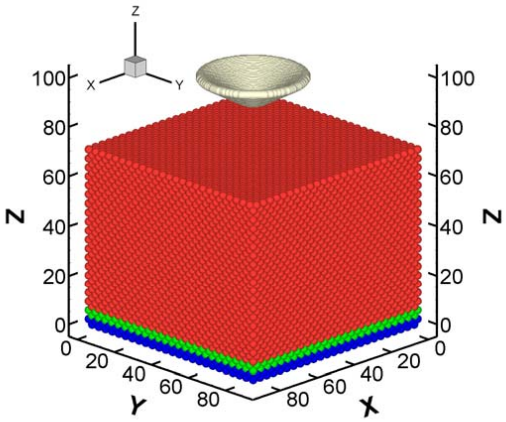

Figure 3: MD model used in nanoindentation tests.

3 ANN indentation model

The objective of the MD simulations described above is to determine the resultant force acting on the indenter tip at each value of the tip displacement in order to construct the corresponding load-displacement curve under each of the considered

testing temperatures. The load data are then input to a suitably trained artificial neural network (ANN) in order to inversely derive the corresponding stress-strain curve such that the mechanical properties of the thin film can be extracted. The ANN is trained using the data obtained from a FE analysis of the nanoindentation process. Figure 4 presents a schematic illustration of the 2-D axisymmetric finite element model constructed using the conventional ABAQUS finite element solver. Note that in the FE simulations, the nodes at the base of the model were prevented from moving in the x- or y-directions, while the nodes along the axisymmetric axis were constrained in the x-direction. As in the MD simulations, the FE analysis considers a conical indenter with a tip radius of 10 Å and a half-angle of 60°. The thickness of the copper film is again specified as 72.3 Å. The FEM analysis simulated the indentation process over both the loading and the unloading stages similar as MD simulation. During the loading process, the indenter was pushed into the copper substrate using a displacement control mechanism and the changing depth is monitored. For a given displacement, the corresponding load at each incremental depth was computed from the reaction force acting on the indenter. The copper film was assumed to experience an incremental plasticity effect with isotropic hardening during the indentation process, and its behavior was modeled using the following constitutive equation:

$$\sigma = E\varepsilon, \text{ for } \varepsilon \leq S_y/E \quad \sigma = E_t\varepsilon + (1 - E_t/E)\,S_y, \text{ for } \varepsilon > S_y/E \tag{3}$$

where E , S_y and E_t are material constants and σ and ε are the stress and strain, respectively. Note that the elastic modulus E can be obtained from the results of MD nanoindentation simulation.

Figure 5 illustrates the topography of the feed-forward ANN used in the present study to derive the material properties of the thin copper film. As shown, the network comprises an input layer, two hidden layers and an output layer. The input variables (F_n) represent the reaction force acting on the indenter during the indentation process and are obtained initially by discretizing the load-displacement curve obtained in the FE simulation using a uniform displacement interval. Meanwhile, the outputs of the ANN are the two material constants of the constitutive model given in Eq. 3, i.e. S_y and E_t. Before the ANN can be used to predict the values of S_y and E_t from an input set of force data,F_n, it must first be trained to ensure the accuracy of the prediction results. As shown in Figure 5, each neuron in a given layer of the ANN has a weighted connection to every neuron in the layer above it. The objective of the training process is to adaptively adjust the weights of these connections such that the network outputs the expected values of S_y and E_t for any given set of input force data. In practice, this is achieved by creating a large training set comprising matched pairs of input data (F_n) and known output data (S_y and

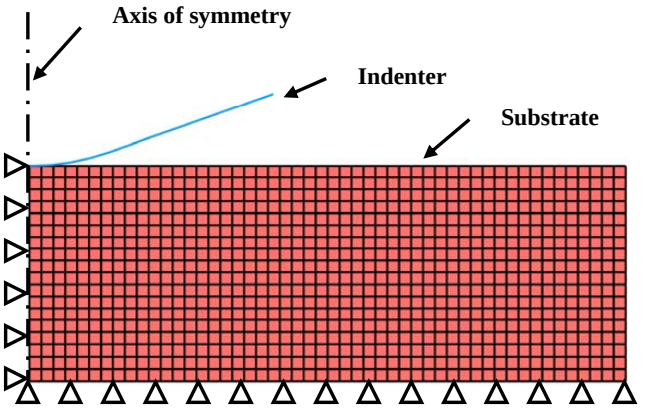

Figure 4: Finite element mesh used to model indentation process. (Note corresponding boundary conditions are also shown).

E_t) and then using a backpropagation scheme to iteratively adjust the values of the weighted connections based upon a minimized mean square error (MSE) criterion such that the actual output values of the ANN for any set of input data converge toward the known values associated with this particular set of input data. Having trained the ANN, a final verification procedure is performed using a further sets of input-output data not included within the original training set.

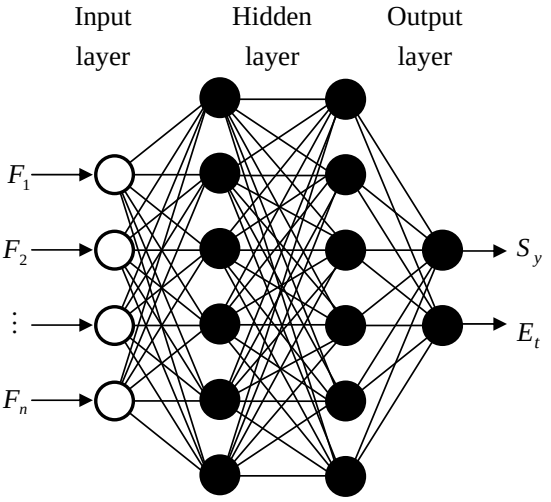

Figure 5: Topography of ANN used to derive material constants from load data.

From the preceding discussions, it follows that the trained ANN will yield a poor predictive performance when presented with input data which fall outside the domain of the original training data. Thus, a careful selection of the training data is required to ensure that the ANN successfully generalizes the indentation response of the thin film under the particular nanoindentation conditions considered in the present MD simulations. As will be discussed later, this is achieved in the current study by ensuring that the domain of the FEM data used to train the ANN fully encompasses that of the MD simulation results.

4 MD simulation results

The validity of the self-written MD code was confirmed by simulating the nanoindentation of the copper substrate at a temperature of 900 K and comparing the results with the simulation data presented in [Hsieh, Ju, Li and Hwang (2004)]. The corresponding load-displacement curves are presented in Figure 6. Note that in the simulations, the load acting on the diamond indenter was obtained by summing the resultant forces contributed by the surrounding copper atoms in the z-direction. It is observed that a reasonable qualitative agreement exists between the two sets of results, and thus the validity of the MD code is confirmed.

Having confirmed the validity of the MD code, nanoindentation simulations were performed using a conical indenter with a tip radius of 10 Å and a half-angle of 60° at temperatures of 300 K, 600 K, 900 K and 1400 K, respectively. The corresponding load-displacement curves are presented in Figure 7; and deformed shape after indentation at the temperature of 300 K is illustrated in Figure 8. Overall, the results show that for a given indentation depth, the applied load decreases as the temperature increases. In other words, the substrate material exhibits a softening effect at higher temperatures. Utilizing these load-displacement curves, the elastic modulus of the copper film at each of the test temperatures was estimated using the method presented by Oliver and Pharr (1992). The results presented in Figure 9 show that the elastic modulus of the copper substrate varies from 119∼174 GPa over the temperature range of 300∼900 K. These results compare to an elastic modulus range of 150∼220 GPa obtained numerically over an equivalent temperature range in [Hsieh, Ju, Li and Hwang (2004)]. The discrepancy between the two sets of results can most likely be attributed to the thickness of the modeled copper is relatively thin in the reference. Therefore the results in [Hsieh, Ju, Li and Hwang (2004)] could affect by substrate effects. A suggestion is mentioned that the indentation depth must smaller than the 1/5 of the film thickness, indentation depth is generally restricted within 1/10 or 1/7 of film thickness to avoid the influence of substrate.

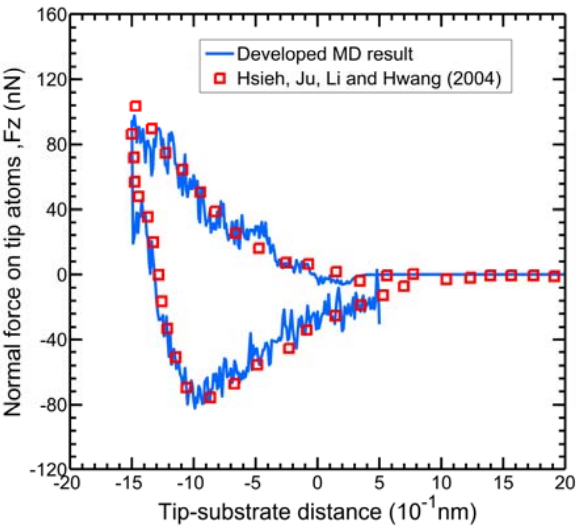

Figure 6: Comparison of MD results and numerical results [Hsieh, Ju, Li and Hwang (2004)] for load-displacement curve of thin copper film indented at 900 K.

5 Inverse analysis results

As described earlier, the ANN was trained (and its performance verified) using the data obtained from FE simulations of the nanoindentation process. By substituting typical elastic modulus values obtained from the MD results into Eq. (3), the assumption of perfect plastic model ($E_t = 0$) is adopted for each training set. Note that at each specific temperature has 20 pairs of data with equivalent spacing for S_y, the spacing regime are listed in Table 2. Figure 10 compares the load-displacement curves obtained from the FE model using these parameter values with those obtained from the MD simulations at each of the considered test temperatures. It is evident that the FE load-displacement curves encompass all of the MD load-displacement profiles, and thus the load data corresponding to these FE curves represent suitable data with which to train the ANN. As discussed earlier, the training data were obtained by discretizing the FEM load-displacement curves shown in Figure 10 using a uniform displacement interval. Having trained and verified the ANN, the load data obtained in the MD simulations at each of the test temperatures were provided as inputs to the ANN to compute the corresponding values of S_y. These material constants were then used to construct the corresponding

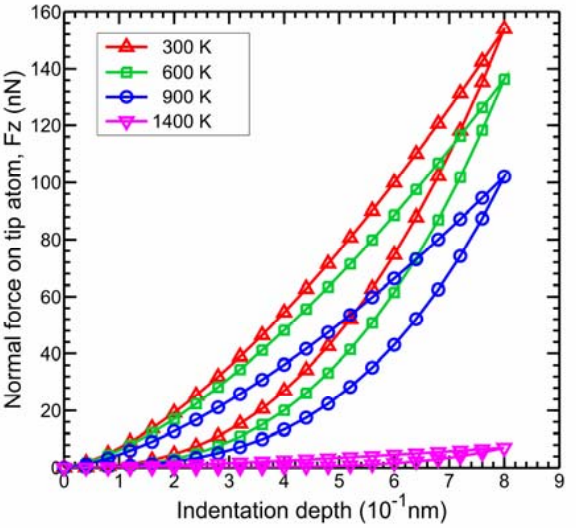

Figure 7: MD simulation results obtained for load-displacement curves of thin copper film at temperatures ranging from 300∼1400 K.

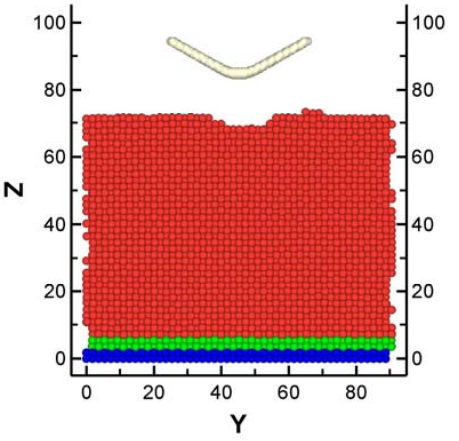

Figure 8: Atomic configuration of copper substrate after nanoindentation at temperature 300 K.

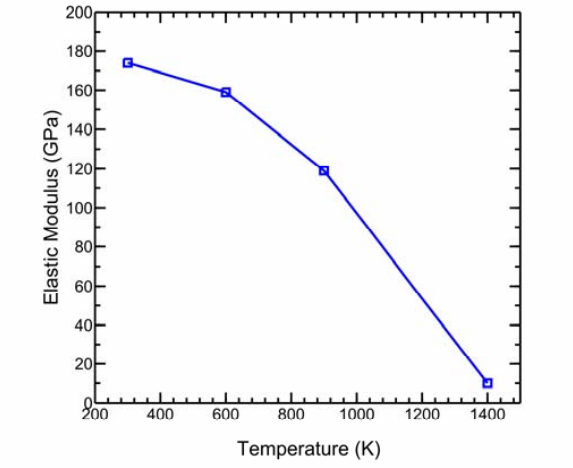

Figure 9: Atomic configuration of copper substrate after nanoindentation at temperature 300 K.

stress-strain curves. Figure 11 presents the inversely-derived stress-strain curves at each of the four test temperatures considered in the MD simulations. Note that the stress-strain curves computed directly from the FEM load-displacement curves shown in Figure 11 are also shown for comparison purposes. A snapshot of the maximum deformed shape and Von Mises stress contour at the temperature of 300 K is presented in Figure 12.

Table 2: Material properties used in training ANN

Temperature (K)	300	600	900	1400
S_y(GPa)	1∼20	0.5∼10	0.5∼10	0.05∼1

Figure 13 illustrates the reduction ratio of the elastic modulus and plastic level, respectively, over the considered temperature range of 300∼1400 K. From inspection, it is determined that the elastic modulus varies in the range of 10∼174 GPa, while the plastic level varies from 0.3∼8.5 GPa. Note that the reduction ratio at any temperature is computed simply by dividing the corresponding value of the material property by the value of the property at a temperature of 300 K (i.e. 174 GPa or 8.5 MPa, as appropriate). From an inspection of Figure 13, it is found that the elastic modulus and plastic level both reduce more than 30% of their original values as the temperature is increased from 300 K to 900 K. As the system temperature

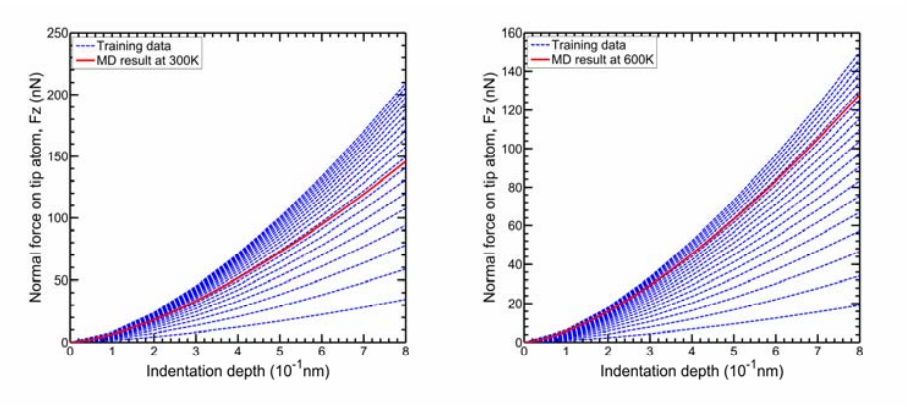

(a) (b)

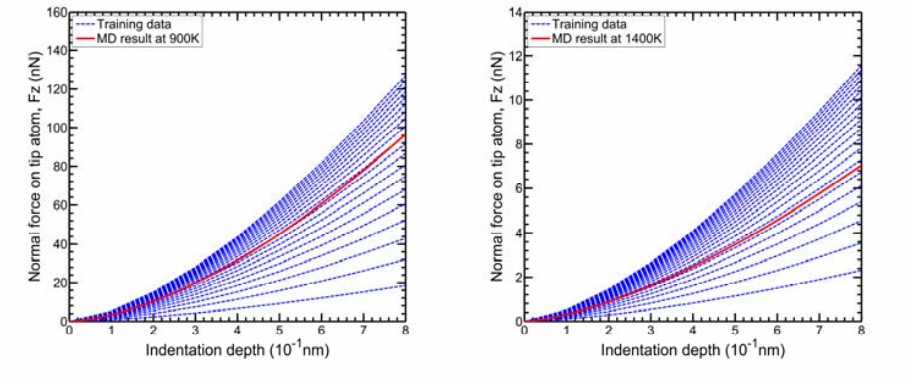

(c) (d)

Figure 10: FE load-displacement curves used for ANN training and MD results at (a) 300 K, (b) 600 K, (c) 900 K, (d) 1400 K.

approaches the melting point of copper (1357.77 K), the thin film changes from a solid to a liquid state, resulting in a significant loss of strength, as shown in Figure 14.

The value of 174 GPa obtained from the MD simulation for the elastic modulus of copper at a temperature of 300 K compares to a value of 145 GPa for copper film by direct nanoindentation measurements at room temperature [Pelletier, Krier, Cornet and Mille (2000)]. In other words, the inversely-derived value of the elastic modulus of the perfect, defect-free monocrystalline thin copper film is around

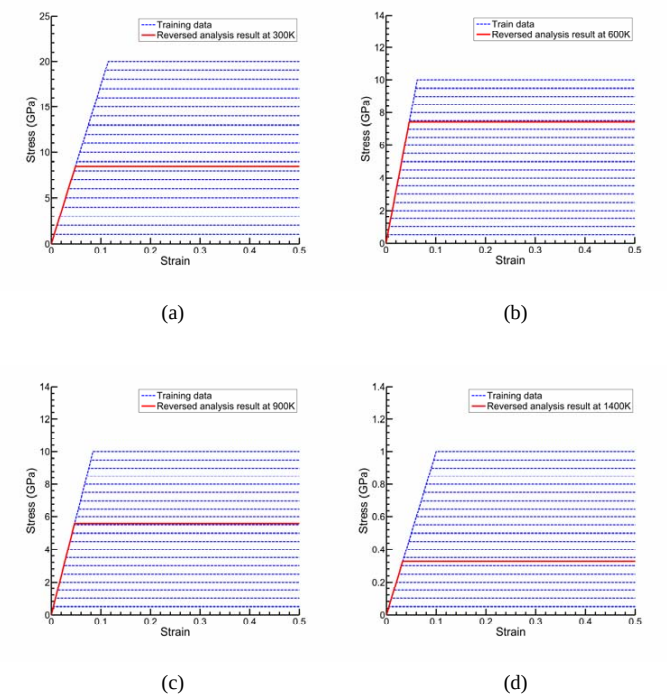

Figure 11: FE stress-strain curves used for ANN training and inversely-derived results at (a) 300 K, (b) 600 K, (c) 900 K, (d) 1400 K.

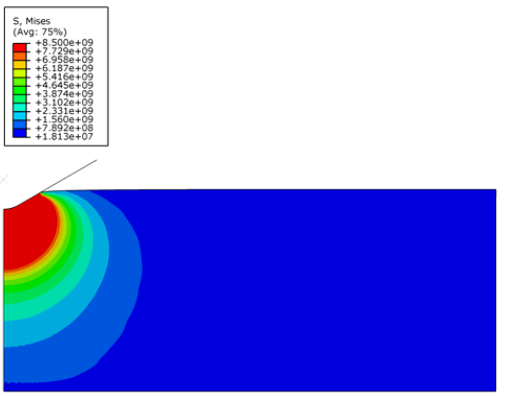

Figure 12: The maximum deformed shape and Von Mises stress contour of copper substrate at the temperature of 300 K.

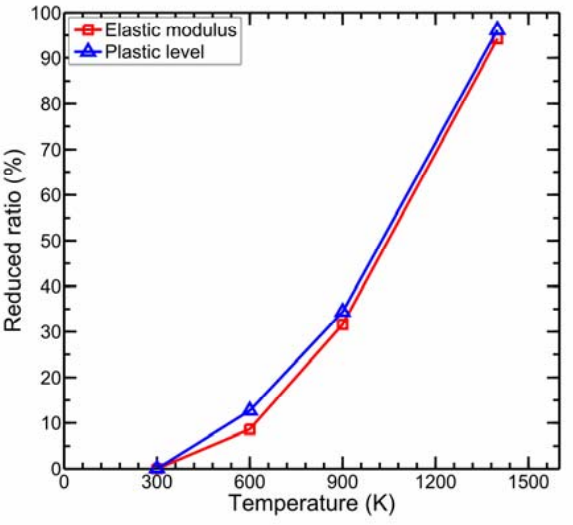

Figure 13: Variation of elastic modulus and plastic level and corresponding reduction ratio over considered temperature range.

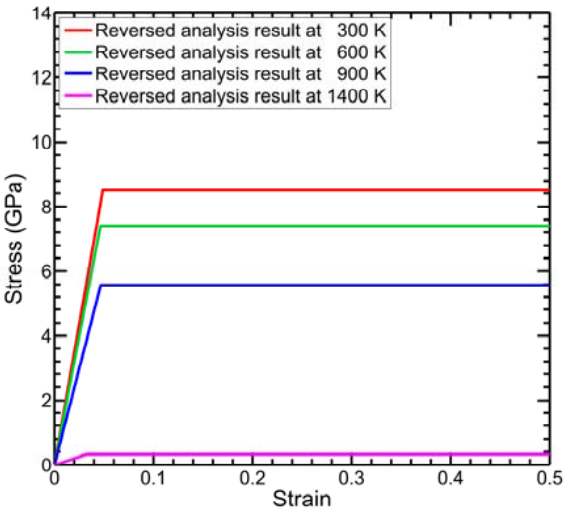

Figure 14: Inversely-derived stress-strain results at temperatures ranging from 300∼1400 K.

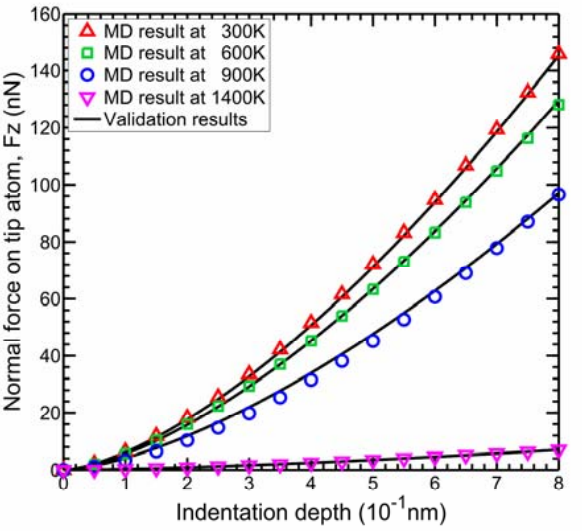

Figure 15: Comparison of FE load-displacement curves based on stress-strain data inversely derived by ANN model and MD load-displacement curves.

120% higher than that of the bulk material. In the previous studies, the authors also found the MD-simulated elastic modulus of copper thin film (220 GPa) is approximately 146% large than the micro-experimental elastic modulus (150 GPa) [Hsieh, Ju, Li and Hwang (2004)]. This discrepancy is a result of the scale differences between experiment and simulation, the former being at a microscale, the latter being at an atomistic scale. An additional reason for the observed discrepancy was the simulation's assumption of a perfect defect-free monocrystalline films and the experimental specimens were polycrystalline and contained a variety of defects.

The validity of the inversely-derived stress-strain curves can be confirmed by using the associated stress-strain data to recreate the corresponding FE load-displacement curves and then comparing these curves with those obtained from the MD simulations. The corresponding results are shown in Figure 15. Good agreement exists between the two sets of results in every case. The correctness of inversely-derived stress-strain curves has been verified.

6 Conclusion

This study has proposed a novel method for estimating the temperature-dependent elasto-plastic properties of a nanoindented thin film. In the proposed approach, MD

simulations of the nanoindentation process are performed at various temperatures. The resulting load-displacement curves are then used to identify suitable conditions under which to perform FE simulations of the nanoindentation process. The load data and material constants obtained from the FE simulations are then used to train an ANN such that for any given set of load data, the network predicts the corresponding values of the material constants. These material constants are used to construct the stress-strain curve, from which the elastic modulus and plastic level of the indented material are then derived. Finally, the validity of the inversely-derived stress-strain curves is confirmed and the results show that a good agreement exists in load-displacement curves for nanoindentation process. In summary, the method presented in this study provides a novel approach for determining the thermal mechanical constitutive model of a nano-thickness metallic thin-film. The analyzed procedure can be applied to most of thin film materials which have the suitable potential function in MD simulation. The resulting temperature-dependent stress-strain curves provided the crucial requirement for quantitative study of nanofabrication process such as nanoimprint lithography and nanoelectromechanical systems.

Acknowledgement: The authors would like to thank the National Science Council of the Republic of China, Taiwan, for financially supporting this research under Contract No. NSC 96-2221-E-194-026 and NSC97-2221-E-194-021-MY3.

Reference:

Bouzakis K. D.; Vidakis, N. (1999): Superficial plastic response determination of hard isotropic materials using ball indentations and a FEM optimization technique. *Materials Characterization*, vol. 42, no. 1, pp. 1–12.

Bouzakis, K. D.; Michailidis, N.; Erkens, G.. (2001): Thin hard coatings stress–strain curve determination through a FEM supported evaluation of nanoindentation test results. *Surface and Coatings Technology*, vol. 142–144, pp. 120–109.

Bouzakis, K. D.; Michailidis, N.; Hadjiyiannis, S.; Skordaris, G.; Erkens, G.: (2003): The effect of specimen roughness and indenter tip geometry on the determination accuracy of thin hard coatings stress–strain laws by nanoindentation. *Materials Characterization*, vol. 49, no. 2, pp. 149–156.

Chen, J.; Yuan, H.; Wittmann, F. H. (2002): Computational Simulations of Micro-Indentation Tests Using Gradient Plasticity. *CMES: Computer Modeling in Engineering & Sciences*, vol. 3, no. 6, pp. 743–754.

Fang, T. H.; Weng, C. I.; Chang, J. G. (2003): Molecular dynamics analysis of temperature effects on nanoindentation measurement. *Materials Science and Engineering A*, vol. 357, no. 1–2, pp. 7–12.

Fang, T. H.; Chang, W. J.; Weng, C. I. (2006): Nanoindentation and nanomachining characteristics of gold and platinum thin films. *Materials Science and Engineering A*, vol. 430, no. 1–2, pp. 332–340.

Haile, J. M. (1992): *Molecular dynamics simulation elementary methods*. John Wiley and Sons, New York.

Hsieh, J. Y.; Ju, S. P.; Li, S. H.; Hwang, C. C. (2004): Temperature dependence in nanoindentation of a metal substrate by a diamondlike tip. *Physical Review B*, vol. 70, no. 19, 195424.

Jayaraman, S.; Hahn, G. T.; Oliver W. C.; Rubin C. A.; Bastias, P. C. (1998): Determination of monotonic stress-strain curve of hard material from ultra-low-load indentation tests. *International Journal of Solids and Structure*s, vol. 35, no. 5–6, pp. 365–381.

Li, J.; Yip, S. (2002): Atomistic measures of materials strength. *CMES: Computer Modeling in Engineering & Sciences*, vol. 3, no. 2, pp. 219–227.

Liang, H.; Woo, C.H.; Huang, H.; Ngan, A. H. W.; Yu, T.X. (2004): Crystalline plasticity on copper (001), (110), and (111) surfaces during nanoindentation. *CMES: Computer Modeling in Engineering & Sciences*, vol. 6, no. 1, pp. 105–114.

Liu, C.L.; Fang, T. H.; Lin, J. F. (2007): Atomistic simulations of hard and soft films under nanoindentation. *Materials Science and Engineering A*, vol. 452–453, pp. 135–141.

Maekawa, K.; Itoh, A. (1995): A friction and tool wear in nano-scale machining - A molecular dynamics approach. *Wear*, vol. 188, pp. 115–122.

Nair, A. K.; Farkas, D.; Kriz, R. D. (2008): Molecular dynamics study of size effects and deformation of thin films due to nanoindentation. *CMES: Computer Modeling in Engineering & Sciences*, vol. 24, no. 3, pp. 239–248

Oliver, W. C.; and Pharr, G. M. (1992): An improved technique for determining hardness and elastic modulus using load and displacement sensing indentation experiments. *Journal of Materials Research*, vol. 7, no. 6, pp. 1564–1583.

Pelletier, H.; Krier, J.; Cornet, A.; Mille, P. (2000): Limits of using bilinear stress-strain curve for finite element modeling of nanoindentation response on bulk materials. *Thin Solid Films*, vol. 379, no. 1–2, pp. 147–155.

Yu, H.; Adams, J. B.; Hector, L. G., Jr. (2002): Molecular dynamics simulation of high-speed nanoindentation. *Modelling and Simulation in Materials Science and Engineering*. vol. 10, no. 3, pp. 319–329.